Supplementary Information

Differential-targeting core-shell microneedle patch with coordinated and prolonged releases of mangiferin and MSC-derived exosomes for scarless skin regeneration

Shang Lyu[a,b,c], Qi Liu[a,b], Ho-Yin Yuen[a,b], Huizhi Xie[d], Yuhe Yang[a,b,e], Kelvin Wai-Kwok Yeung[d], Chak-yin Tang[f], Shuqi Wang[g,h], Yaxiong Liu[i], Bin Li[j,k]*, Yong He[c,]*, Xin Zhao[a,b,e]*

[a] Department of Biomedical Engineering, The Hong Kong Polytechnic University, Hung Hom, Hong Kong SAR 999077, China

[b] Department of Applied Biology and Chemical Technology, The Hong Kong Polytechnic University, Hung Hom, Hong Kong SAR 999077, China

[c] State Key Laboratory of Fluid Power and Mechatronic Systems, School of Mechanical Engineering, Zhejiang University, Hangzhou, Zhejiang 310027, China

[d] Department of Orthopaedics and Traumatology, Li Ka Shing Faculty of Medicine, The University of Hong Kong, Hong Kong SAR 999077, China

[e] The Hong Kong Polytechnic University Shenzhen Research Institute, Shenzhen, Guangdong 518057, China

[f] Department of Industrial & Systems Engineering, The Hong Kong Polytechnic University, Hung Hom, Hong Kong SAR 999077, China

[g.] Tianfu Jincheng Laboratory, City of Future Medicine, Chengdu 641400, China

[h.] College of Biomedical Engineering, Sichuan University, Chengdu 610065, China.

[i] Jihua Laboratory, Foshan, Guangdong 528000, China

[j] Medical 3D Printing Center, Orthopedic Institute, Department of Orthopaedic Surgery, The First Affiliated Hospital, School of Biology & Basic Medical Sciences, Suzhou Medical College, Soochow University, Suzhou, Jiangsu 215006, China

[k] Collaborative Innovation Center of Hematology, Soochow University, Suzhou, Jiangsu 215006, China

* Corresponding author.

E-mail address: binli@suda.edu.cn (B. Li), yongqin@zju.edu.cn (Y. He), xin.zhao@polyu.edu.hk (X. Zhao).

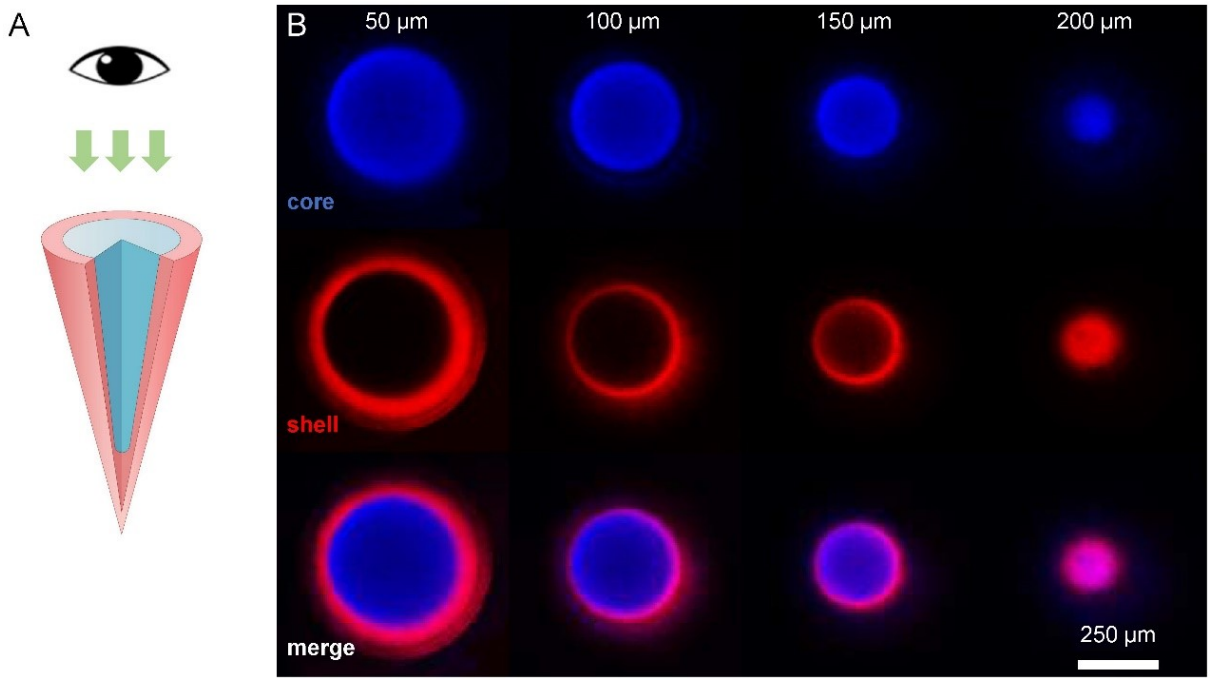

Fig. S1 Confocal images of microneedle structure. (A) Illustration of microneedle observation using confocal microscopy. (B) Confocal images of microneedle cross sections at different height (i.e., 50, 100, 150, 200 μm).

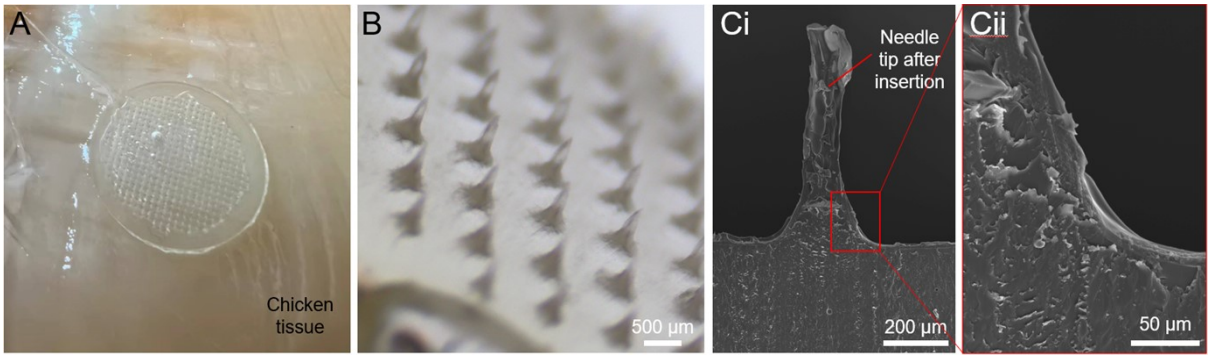

Fig. S2 Core-shell integrity after tissue insertion. (A) The experimental setup image for the tissue insertion test. Chicken tissue was selected as a model to simulate the wound tissue. (B) Microscope image showing the swelling of needle tip after tissue insertion. (Ci) SEM image showing the cross section of the needle tips after tissue insertion. (Cii) Enlarged view showing the interface of P_7L_2DMA-GelMA after tissue insertion.

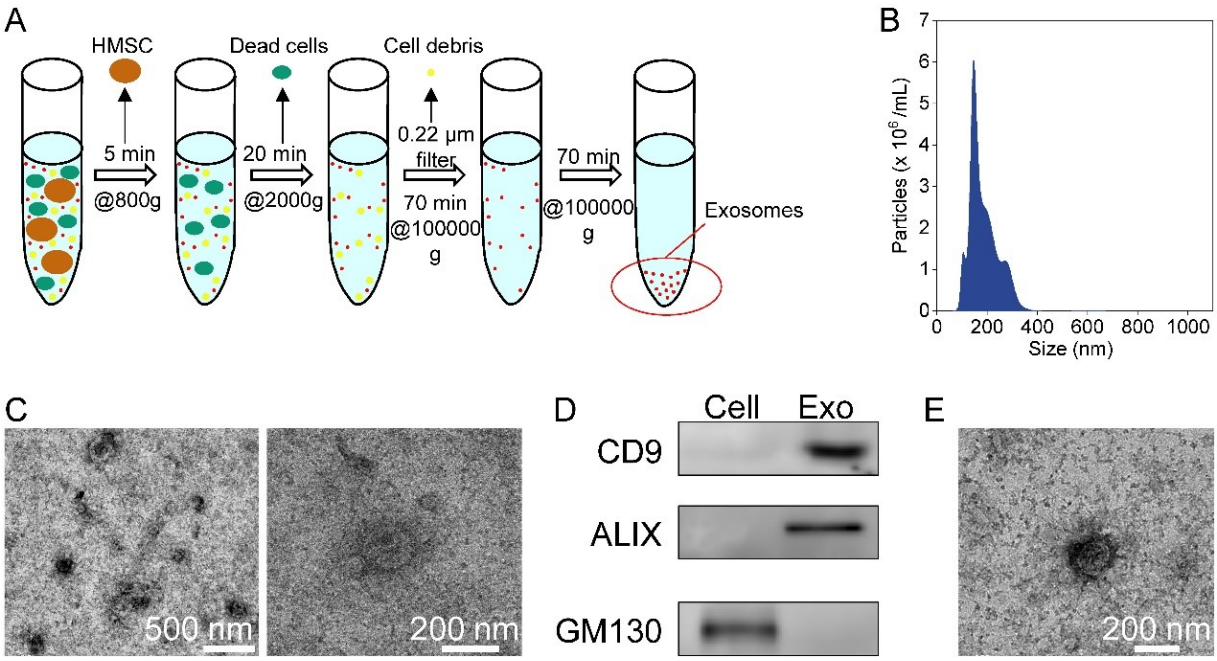

Fig. S3 Extraction and identification of hMSC-derived exosomes. (A) Illustration showing the extraction of hMSC-derived exosomes using differential centrifugation. (B) Nanoparticle tracing analysis of hMSC-derived exosomes. (C) Transmission electron microscope (TEM) images of extracted exosomes prior to loading into P_7L_2DMA. (D) Western blot of representative exosome-related protein markers. Typical exosome marker CD9 and ALIX were expressed while GM130 (Golgi marker) was absent in the extracted exosome, indicating the high purity of the exosomes. (E) TEM images of exosomes after 21-day release from P_7L_2DMA. Similar morphology of exosomes prior to encapsulation and after release indicated that the P_7L_2DMA can preserve the structure of exosomes.

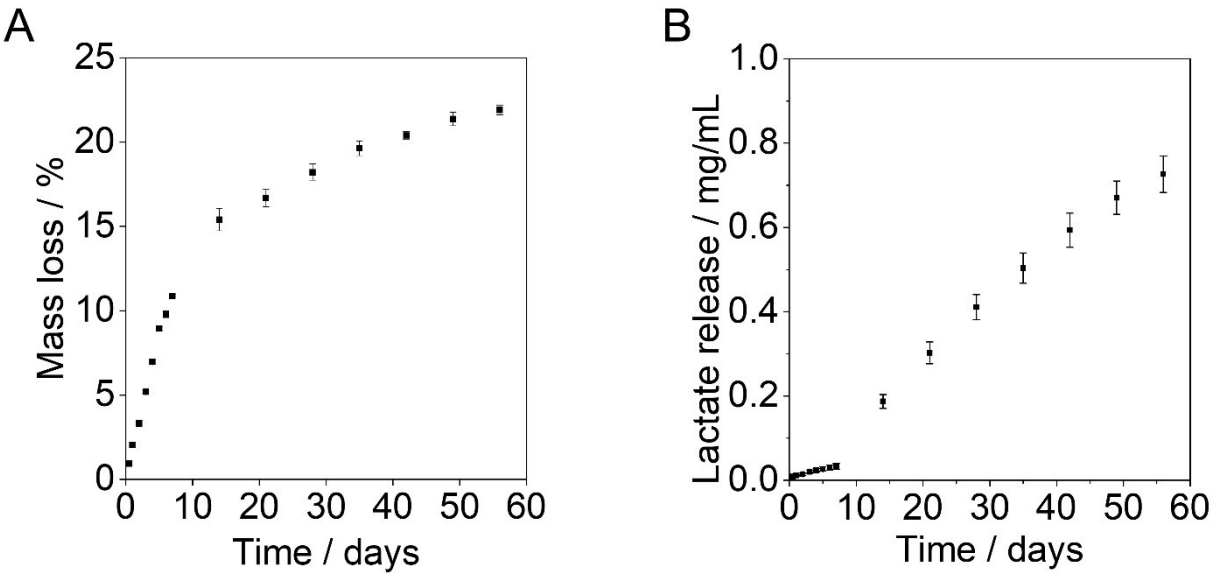

Fig. S4 Degradation of P_7L_2DMA and the main degradation product. (A) Weight loss of P_7L_2DMA after immersion in PBS within 56 days (8 weeks). (B) Cumulative release of Lactate as main degradation product of P7L2DMA after immersion in PBS within 56 days (8 weeks).

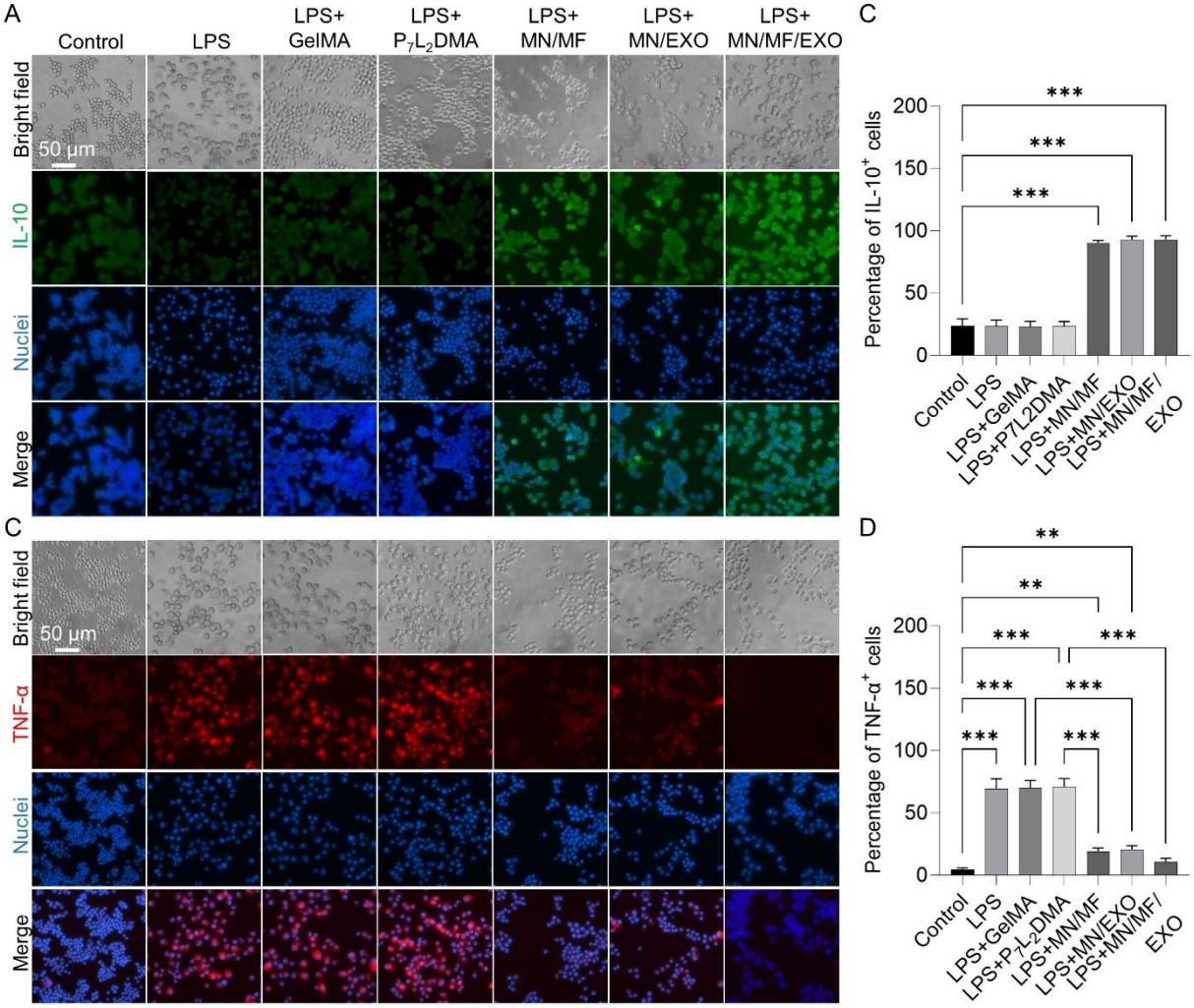

Fig. S5 Anti-inflammatory effect of different components in core-shell microneedles. (A) RAW 264.7 cells cultured in extraction solution of different groups for 48 h marked with IL-10 (green) and DAPI (blue). (B) Quantitative analysis of percentage of IL-10^+ cells in different groups. (C) RAW 264.7 cells cultured in extraction solution of different groups for 48 h marked with TNF-α (red) and DAPI (blue). (D) Quantitative analysis of percentage of TNF-$α^+$ cells in different groups. The differences are statistically significant when p values are below 0.01 (**) and 0.001 (***).

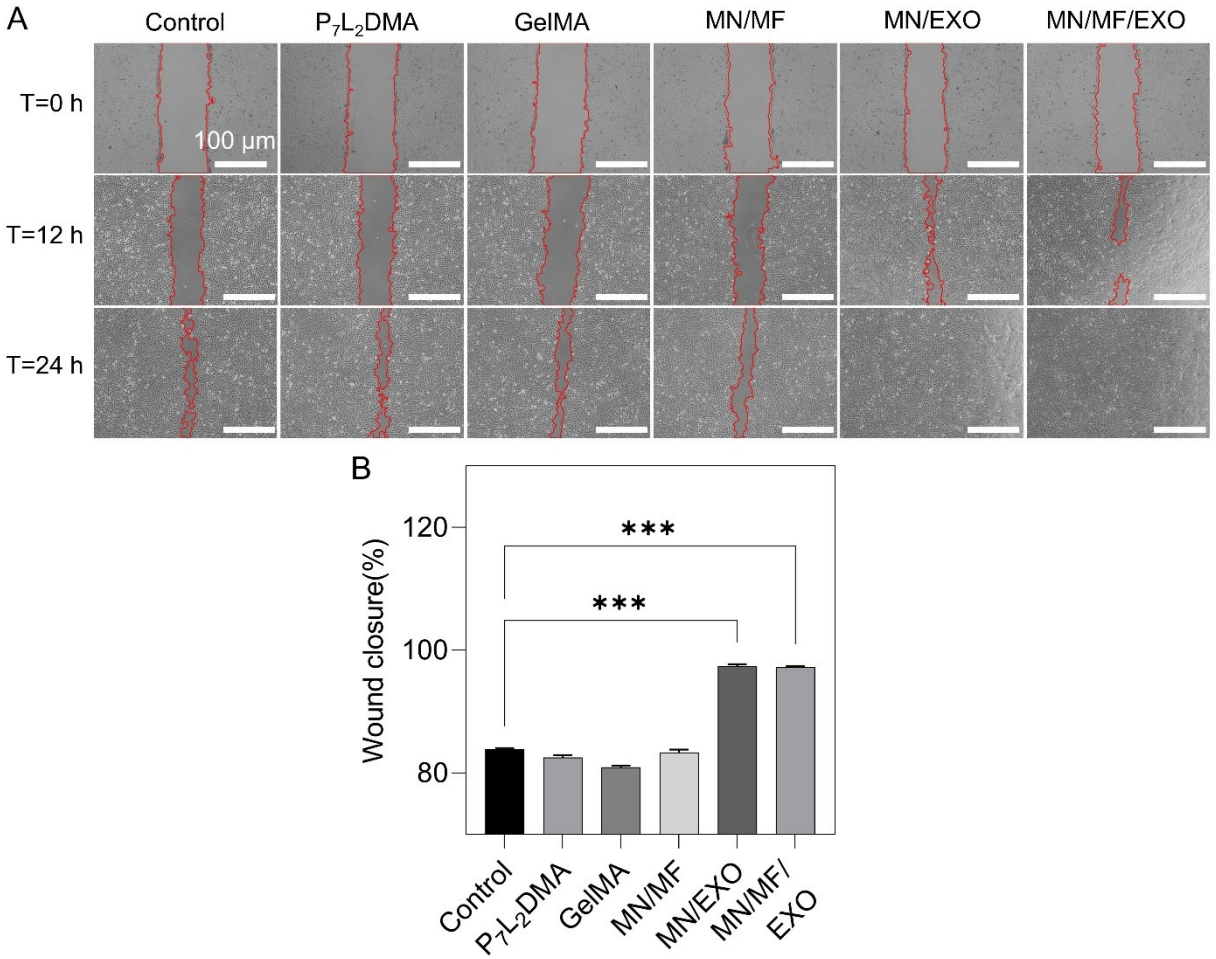

Fig. S6 *In vitro* wound healing effect of different components in microneedles based on HUVECs. (A) Representative bright-field images of HUVECs cultured in extracts from different groups at different time points (0, 12, 24 h) (red lines indicate wound borders). (B) Quantitative analysis of wound closure rate in different groups at 12 h using ImageJ. The differences are statistically significant when p values are below 0.001 (***).

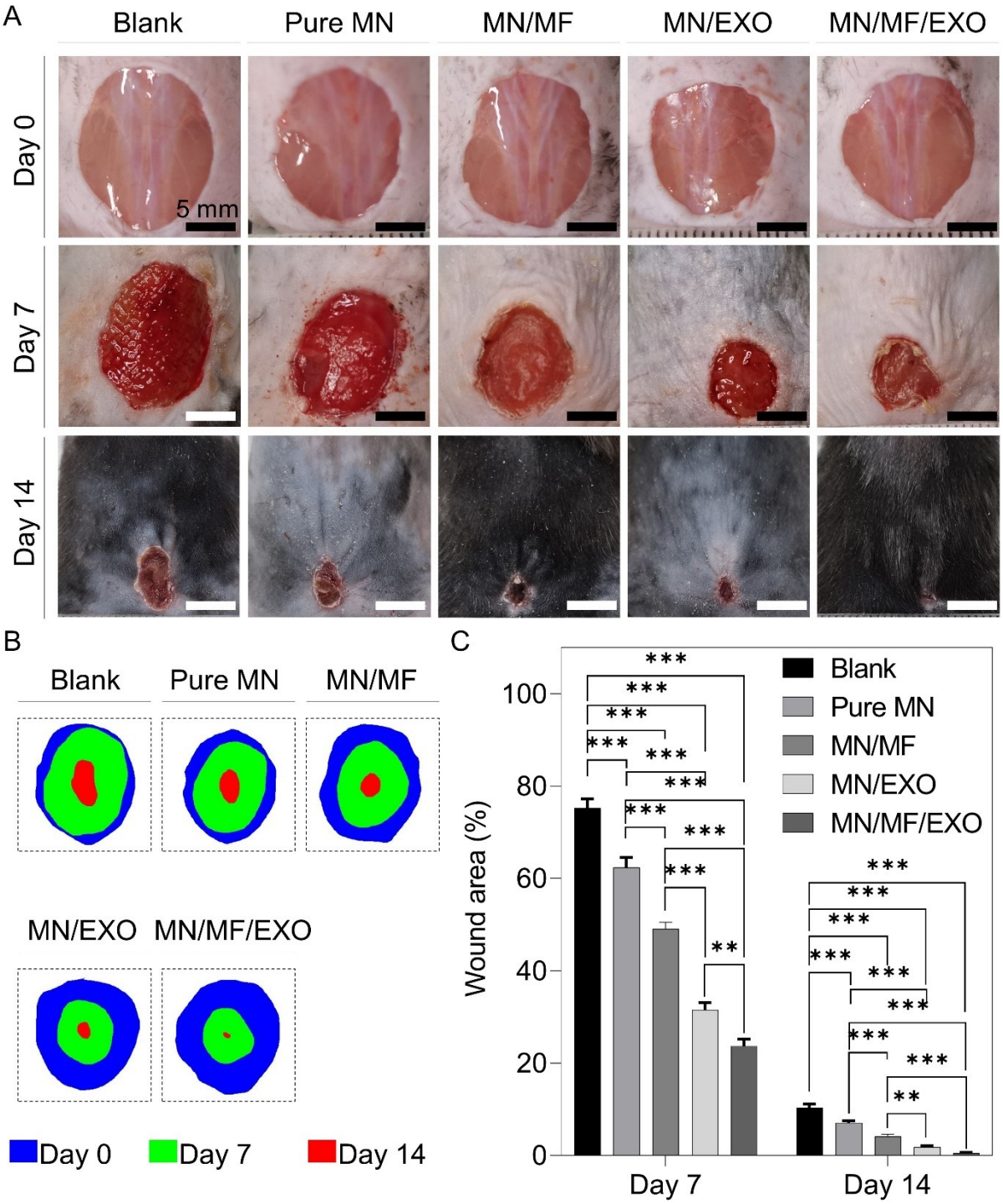

Fig. S7 Assessment of wound closure rate. (A) Images of wound healing in different groups: Blank, pure MN, MN/MF, MN/EXO, and MN/MF/EXO on day 0, 7, and 14. Scale bar, 5 mm. (B) Diagrams of wound area at different time points. Blue, green, and red indicate day 0, 7 and 14, respectively. (C) Quantitative analysis of wound area of different groups on day 7 and 14. The differences are statistically significant when p values are below 0.01 (**), and 0.001 (***).

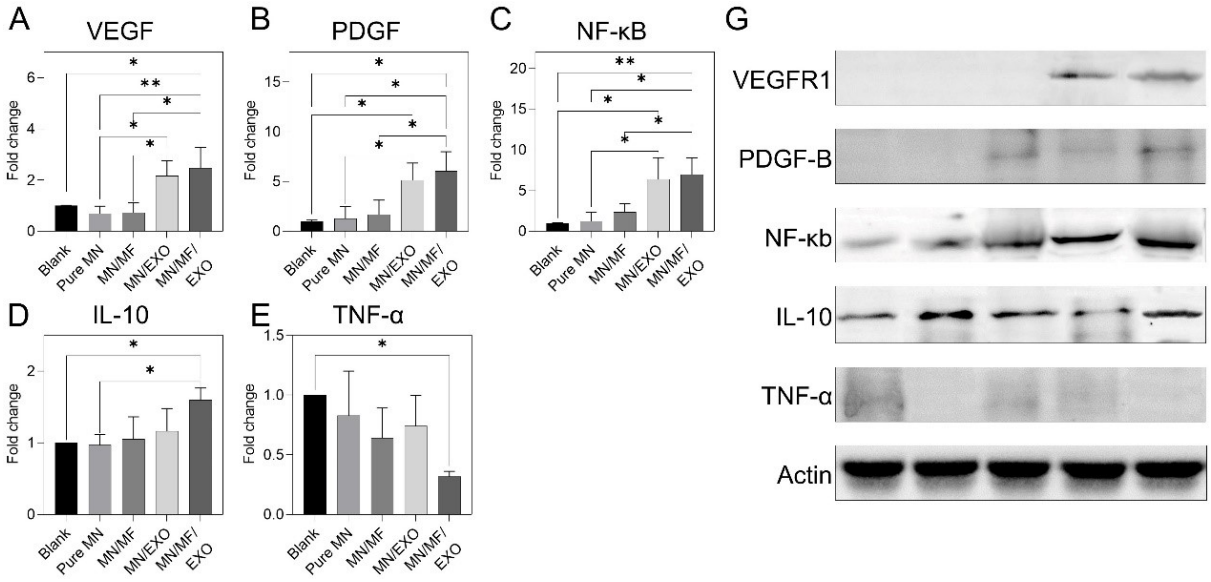

Fig. S8 Inflammation- and angiogenesis-related gene expression in wound bed of different groups. (A)-(F) Real-time quantitative polymerase chain reaction (RT-qPCR) results of vascular endothelial growth factor (VEGF), platelet derived growth factor (PDGF), nuclear factor kappaB (NF-κB), IL-10, and TNF-α expression in wound bed of different groups on day 7. (G) Western blot analysis of VEGFR1, PDGF-B, P65, IL-10, and TNF-α expression in the wound bed of different groups on day 7. The differences are statistically significant when p values are below 0.05 (*) and 0.01 (**).

Fig. S9 Raw data of full gel and blot of CD 9 protein. Supplementary information for Fig. S2D.

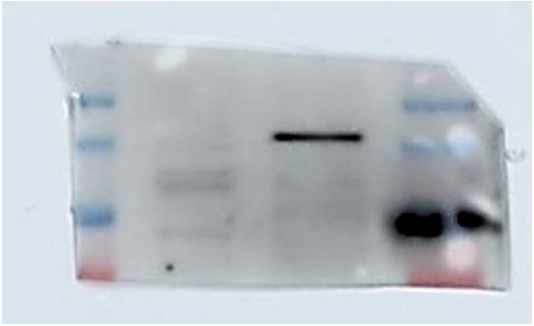

Fig. S10 Raw data of full gel and blot of ALIX protein. Supplementary information for Fig. S2D.

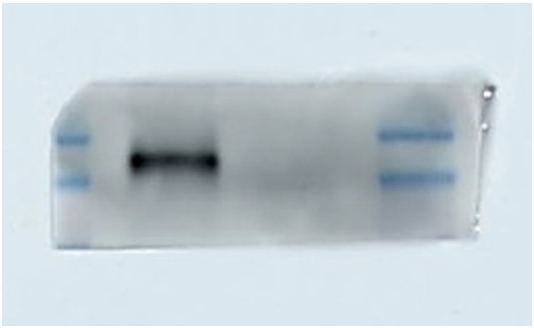

Fig. S11 Raw data of full gel and blot of GM130 protein. Supplementary information for Fig. S2D.

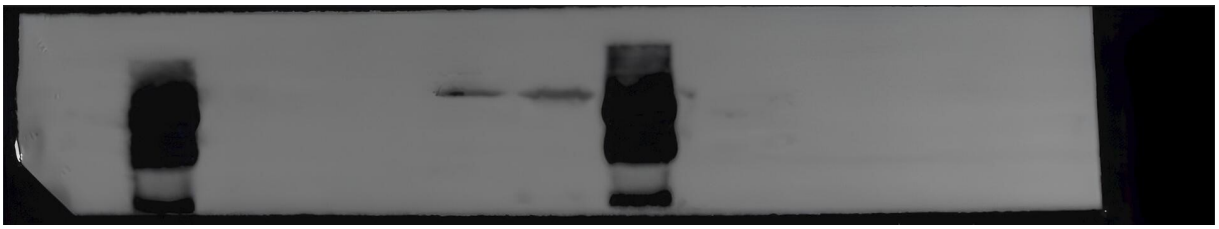

Fig. S12 Raw data of full gel and blot of VEGFR1 protein. Supplementary information for Fig. S6G.

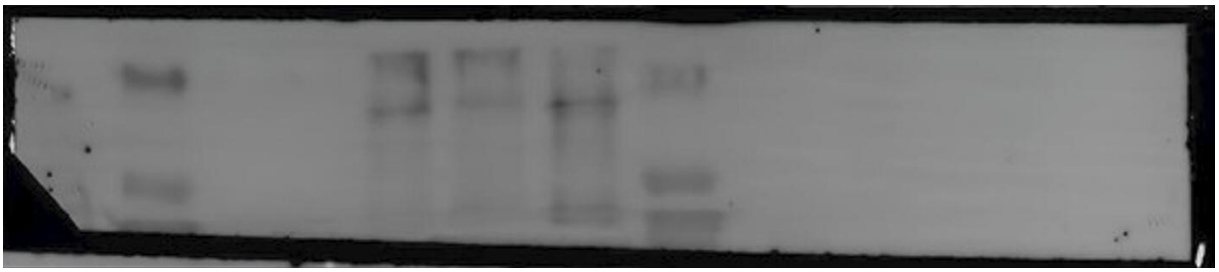

Fig. S13 Raw data of full gel and blot of PDGF-B protein. Supplementary information for Fig. S6G.

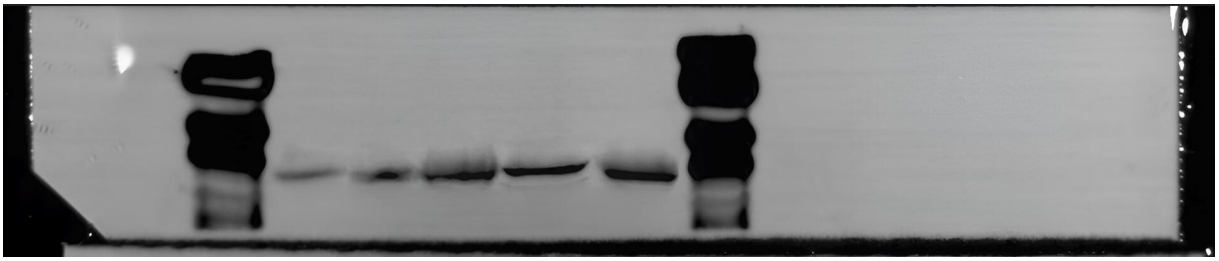

Fig. S14 Raw data of full gel and blot of NF-κB protein. Supplementary information for Fig. S6G.

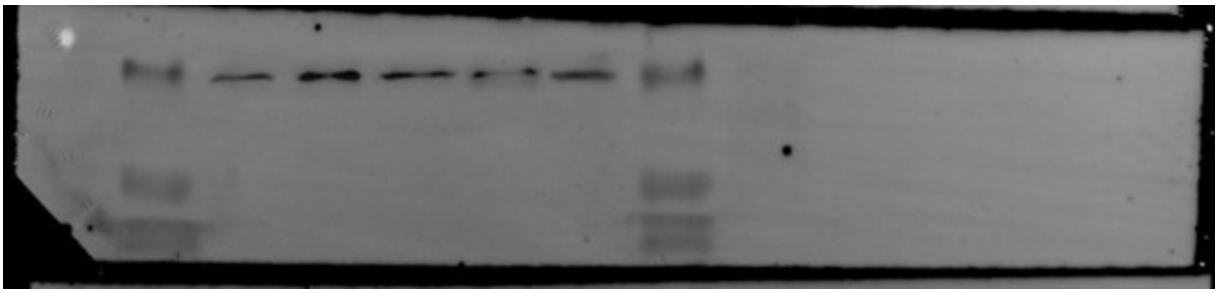

Fig. S15 Raw data of full gel and blot of IL-10 protein. Supplementary information for Fig. S6G.

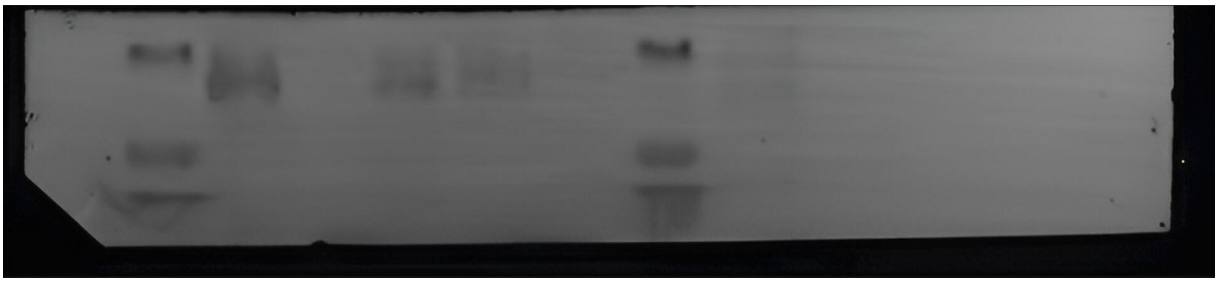

Fig. S16 Raw data of full gel and blot of TNF-α protein. Supplementary information for Fig. S6G.

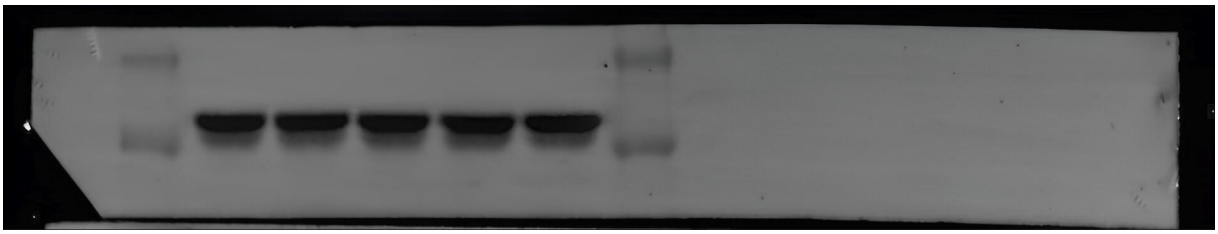

Fig. S17 Raw data of full gel and blot of Actin protein. Supplementary information for Fig. S6G.

Table S1. Abbreviation list for group setting of *in vitro* anti-inflammation, tube formation, and scratch wound healing

Abbreviation	Full name and setting
Control	PBS
LPS	100 ng/mL lipopolysaccharides
GelMA	GelMA extraction
P_7L_2DMA	P_7L_2DMA extraction
MN/MF	100 μg/mL mangiferin loaded GelMA shell/ P_7L_2DMA core microneedle extraction
MN/EXO	GelMA shell/1 mg/mL exosome loaded P_7L_2DMA core microneedle extraction
MN/MF/EXO	100 μg/mL mangiferin loaded GelMA shell/1 mg/mL exosome loaded P_7L_2DMA core microneedle extraction

Table S2. Abbreviation list for group setting of *in vivo* experiment.

Abbreviation	Full name and setting
Blank	PBS
Pure MN	GelMA shell/ P_7L_2DMA core microneedle
MN/MF	100 μg/mL mangiferin loaded GelMA shell/ P_7L_2DMA core microneedle
MN/EXO	GelMA shell/1 mg/mL exosome loaded P_7L_2DMA core microneedle
MN/MF/EXO	100 μg/mL mangiferin loaded GelMA shell/1 mg/mL exosome loaded P_7L_2DMA core microneedle

Table S3. Primers for RT-qPCR

Gene	Forward	Reverse
GAPDH	CCTCGTCCCGTAGACAAAATG	TGAGGTCAATGAAGGGGTCGT
FGF	CCAGGACCAGCTATCACCTACAGA	GCCATTCTCCAGCGTCCACT
IL-10	AATAAGCTCCAAGACCAAGGTGT	CATCATGTATGCTTCTATGCAGTTG
TNF-α	CCCTCACACTCACAAACCACC	CTTTGAGATCCATGCCGTTG
VEGF	GTAACGATGAAGCCCTGGAGTG	TCACAGTGAACGCTCCAGGAT
PDGF	GGCTTATCCGATGCCTTCTGT	TGACTCTCACTCAGCTCCAGCA
NF-κB	CCTGCTTCTGGAGGGTGATG	GGCTCATACGGTTTCCCATTTA